EVALUATION OF A THREE-PHASE DISTRIBUTION SYSTEM STATE ESTIMATION FOR OPERATIONAL USE IN A REAL LOW VOLTAGE GRID

Heiner Früh[1*], Krzysztof Rudion[1],
Alix von Haken[2], Daniel Groß[2], Bartholomäus Wasowicz[2]

[1]Institute of Power Transmission and High Voltage Technology - University of Stuttgart, Stuttgart, Germany
[2]Netze BW GmbH, Stuttgart, Germany
**heiner.frueh@ieh.uni-stuttgart.de*

Keywords: DISTRIBUTION SYSTEM STATE ESTIMATION, REAL MEASUREMENT DATA, METER PLACEMENT, SMART GRID, LOW VOLTAGE

Abstract

The ongoing trend towards active distribution systems formulates a need to know the current state of the system. This information can be generated through a distribution system state estimation (DSSE). The accuracy of DSSE usually suffers from the lack of available measurements. In this paper a three-phase DSSE is performed for a real low-voltage system in Germany. The accuracy of the DSSE is evaluated based on the differences between the measurements and estimation results. Different measurement configurations are analysed, in order to determine a minimal measurement effort required for a given accuracy. Additionally, the optimal placement of new measurement devices is investigated. The results show that the performed DSSE is accurate enough to judge whether the operation of an unmeshed low-voltage system is within its thresholds or not.

1 Introduction

The continuous expansion of decentralised RES in the medium and low-voltage systems and the decommissioning of large power plants in the transmission system as part of the Energy Transition in Germany mean that distribution systems will have to participate in the provision of system services in the future. In order to be able to accomplish the resulting new tasks efficiently and reliably, the DSOs need precise knowledge of the current state of their systems. Future smart grid applications require knowledge of the current system state as well, in order to be adopted into operation. The state estimation (SE) method has been successfully used for this task in the transmission system since the 1970s [1].
However, the different framework conditions, especially the unavailability of measurement values, prevented an immediate adoption to the distribution systems [2]. The asymmetrical operation of distribution systems further increases the complexity. Additionally, the evaluation of distribution system state estimation (DSSE) results during operation in real systems is challenging, because the true system states are not known. One method of validation is to exclude some measurements from the input data of the DSSE and then compare the results of the DSSE with these measurements. However, distribution systems are generally not meshed, but radial. Therefore, the power flows of each feeder are independent from each other and evaluation measurements need to be distributed throughout the whole distribution system.
In this paper, a three-phase DSSE, based on the weighted least squares (WLS) method, is performed for a real low-voltage system in Germany. In addition to high-resolution measurements, pseudo measurements, based on historical data and weather reports, are used as input data. The studies are part of the cooperative research project “Smart Grid Demonstrator” between the Institute of Power Transmission and High Voltage Technology at the University of Stuttgart and the DSO Netze BW GmbH.
One goal of this project is to evaluate the quality of the performed DSSE for a real low-voltage system. The focus is not on the SE algorithms themselves, but on questions regarding their implementation. As one of the key problems of DSSE is the lack of measurements in low and medium voltage systems, this paper tries to find the least expensive measurement setup for a given error margin of the DSSE.

2 Distribution System State Estimation

2.1 State of the Art

There are a number of different methods for DSSE, which are under current research. In [3] the state-of-the-art technologies are reviewed. The challenges, opportunities and future research directions that could facilitate the need of DSSE are discussed in [3] as well. The DSSE methods can be classified into five categories, with the WLS based methods leading in popularity [3].

1. WLS-Based Static DSSE
2. Load Adjustment DSSE Methods
3. Robust DSSE Methods
4. Dynamic DSSE Methods
5. Distributed DSSE Methods

A comparison between a WLS, a Weighted Least Absolute Value (WLAV) and a Schweppe-Huber Generalized-M (SHGM) estimator is performed in [4]. It is concluded that the

WLS estimator produces good and consistent results and is suited for DSSE [4].

A positive influence of Advanced Metering Infrastructure (AMI) on the DSSE accuracy is observed in [5]. The problem of unsynchronised measurements, addressed in [6], is not relevant for this paper, because the used measurement devices are synchronised through the Network Time Protocol (NTP). However, this poses a major obstacle for the implementation of DSSE in future smart grids, utilising only unsynchronised smart meter data.

Even though DSSE is an active research topic there are very little evaluation results of real world DSSE implementations. In [7] DSSE evaluation results for a real medium-voltage feeder are shown. However, it is unclear how the true system states, necessary for the calculation of the DSSE error, are known to the authors of [7]. In [2] the voltage magnitude deviations for a DSSE in a real medium-voltage system are presented. However, the deviations of the current flows could not be calculated in [2], due to the lack of real power flow measurements.

2.2 Basics of WLS State Estimation

In this paper a three-phase WLS based DSSE is evaluated for operational usage in a real low-voltage grid. It uses the complex bus voltages as the state variables and is implemented similar to the DSSE in [2]. The difference is in the usage of state variables in polar, instead of cartesian notation.

The mathematical representation of the WLS based SE problem is given in equation (1).

$$min\,\boldsymbol{J}(\boldsymbol{x}) = [\boldsymbol{z} - \boldsymbol{h}(\boldsymbol{x})]^T \boldsymbol{R}^{-1} [\boldsymbol{z} - \boldsymbol{h}(\boldsymbol{x})] \qquad (1)$$

Equation (1) is the objective function $\boldsymbol{J(x)}$ of the DSSE, where $\boldsymbol{z}$ describes the measurement vector and $\boldsymbol{h(x)}$ the calculated measurement vector based on the current state variable vector $\boldsymbol{x}$. The weighting matrix $\boldsymbol{R}$ depends on the accuracy of the measurement values. To determine the state variables, the objective function is derived for $\boldsymbol{x}$, resulting in equation (2), with $\boldsymbol{H}$ describing the Jacobian matrix.

$$\left[\frac{\partial \boldsymbol{J}(\boldsymbol{x})}{\partial \boldsymbol{x}}\right] = -2\boldsymbol{H}^{\boldsymbol{T}}(\boldsymbol{x})\boldsymbol{R}^{-1}[\boldsymbol{z} - \boldsymbol{h}(\boldsymbol{x})] \qquad (2)$$

In order to minimise equation (2), equation (3) must be satisfied.

$$\boldsymbol{H}^{\boldsymbol{T}}(\boldsymbol{x})\boldsymbol{R}^{-1}[\boldsymbol{z} - \boldsymbol{h}(\boldsymbol{x})] = 0 \qquad (3)$$

Due to the nonlinearity of $\boldsymbol{h(x)}$, it is developed for a linearization in a Taylor series around the start value $\boldsymbol{x_0}$, according to equation (4):

$$\boldsymbol{h}(\boldsymbol{x}) = \boldsymbol{h}(\boldsymbol{x}_0) + \boldsymbol{H}(\boldsymbol{x}_0)\Delta\boldsymbol{x} \qquad (4)$$

Equation (5) is obtained from substituting equation (4) into equation (3).

$$[\boldsymbol{H}^T(\boldsymbol{x}_0)\boldsymbol{R}^{-1}\boldsymbol{H}(\boldsymbol{x}_0)]^{-1}\boldsymbol{H}^T(\boldsymbol{x}_0)\boldsymbol{R}^{-1}[\boldsymbol{z} - \boldsymbol{h}(\boldsymbol{x}_0)] = \Delta\boldsymbol{x} \qquad (5)$$

Equation (5) is the target function of the DSSE and needs to be solved iteratively after Newton-Raphson. The changes of the state variables $\boldsymbol{\Delta x}$ terminate the DSSE, when falling below a predefined threshold [8][9].

3 Methodology

3.1 Case Study

The study is conducted in a rural low-voltage system in Germany over a timespan of one week. The grid is mainly characterised by its high penetration of PV plants. It consists of 52 loads and 30 PV plants, which have a rated power of 480 kWp in total. This leads to peaks in power generation, which are up to seven times higher than the maximum load. The systems total demand of active power, averaged minutely, during the studied period is shown in Fig. 1, highlighting the high generation as well as the noisiness of the data. Fig. 1 illustrates that the sky was clouded during the test period. This reduces the accuracy of estimations of the PV power output based on weather reports significantly, compared to days with clear skies.

An overview of the grid topology is presented in Fig. 2. The grid model of this study accounts for the couplings between the three main phases, but the neutral conductor is not considered, due to the lack of detailed information about the grounding of system components.

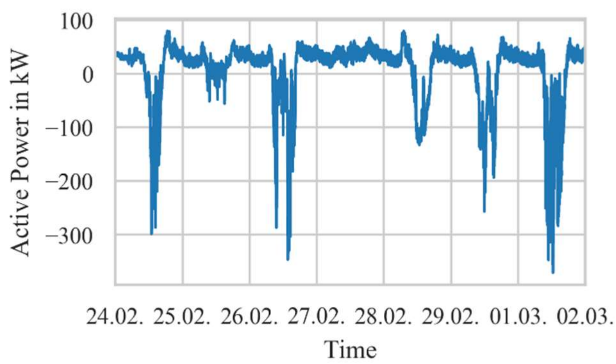

Fig. 1: Minutely averaged active power demand at the low-voltage busbar of all three phases summed up.

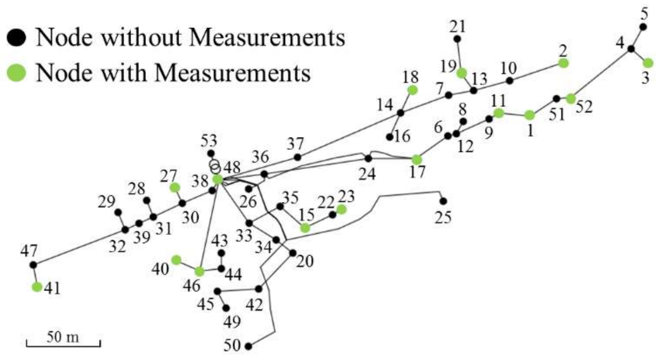

Fig. 2: Grid topology of the real low-voltage system under study and placement of measurement devices.

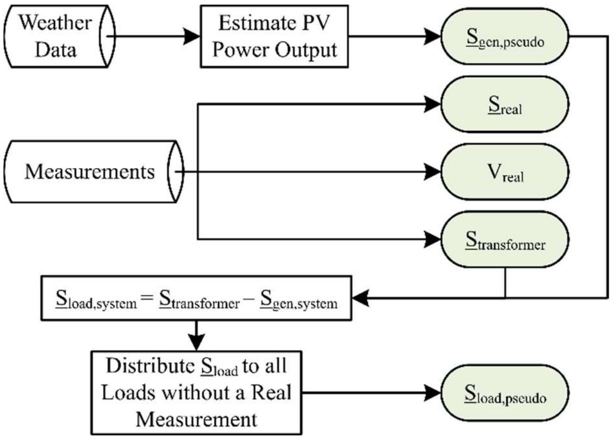

Fig. 3: Flowchart showing the generation of the DSSE input data (rounded boxes).

3.2 Input Data for the DSSE

In order to perform a DSSE, measurement devices are installed at different locations in the grid, as marked in Fig. 2 by the green circles. In addition to the low-voltage busbar of the transformer (node 48), all outgoing connections to the individual feeders of the grid are measured as well. The relevant measurements for the scope of this paper are the voltage and current magnitudes as well as the signed values of the active and reactive power. All measurements are ten period RMS values for each of the three main phases of the low-voltage system, which are collected in a time interval of one second.

As it is unlikely that such high-resolution data will be available for low-voltage systems in the near future, the data used in this paper was aggregated to one-minute average values.

However, the amount of available measurements is not enough to perform a DSSE, because not every node in the grid is equipped with a measurement device. Therefore, pseudo measurements are used as input data as well. These pseudo measurements are derived from the power flow measurements at the transformer in combination with an estimation of the total generated power of the system. From these data the systems total power demand is calculated and distributed among the unmeasured loads. The flowchart in Fig. 3 explains this process, if only the transformer data itself is considered. If the power flow measurements of each feeder are considered as well, the process is adapted accordingly.

3.3 Evaluation of the DSSE Results

Because the true system states are unknown, the evaluation of the DSSE results is based on the deviations to all available measurements. The deviations of the voltage magnitudes are calculated relative to the nominal voltage, according to equation (6). The calculation of the current magnitude deviations is relative to the rated current of each line, according to equation (7).

$$V_{dev} = \frac{|V_{mes}| - |\underline{V}_{DSSE}|}{|V_n|} \cdot 100\% \tag{6}$$

$$I_{dev} = \frac{|I_{mes}| - |\underline{I}_{DSSE}|}{|I_{rated}|} \cdot 100\% \tag{7}$$

The nominal voltages V_n and rated currents I_{rated} are chosen as reference values, because they can also be used to describe the thresholds of the system. E.g. a value of I_{dev} = 1% can easily be judged unproblematic, because the normal operation of the system is not endangered by this inaccuracy of the estimation. A deviation range of ±1% is defined for V_{dev} as the DSSE accuracy target. For the current magnitudes a range of ±3% is chosen for each phase of the system. This results in an inaccuracy of less than 10% of the line loadings, for the worst case of constructive superposition of the deviations.

It is assumed that it is possible to judge whether the operation of a distribution system is within its thresholds or not, based on the results of a DSSE within these deviation ranges. The highest currents are usually observed at the transformer and the first line of each feeder. Together with all the voltage magnitudes, they describe the critical values of the system operation. Therefore, the results presented in this paper will focus on these values.

3.4 DSSE Scenarios

In order to evaluate the DSSE and to find a cost-effective measurement setup, different scenarios are investigated. All of these scenarios are based on a minimal measurement setup.

3.4.1 Sc. 1 - Base Scenario: this scenario utilises only the measurements recorded at the low-voltage busbar of the transformer. The rest of the DSSE input data are pseudo measurements, which are determined according to Fig. 3.

3.4.2 Sc. 2 - Feeder Measurements: in addition to the measurements at the low-voltage busbar of the transformer, the power flow measurements of each feeder are used as input data as well. The pseudo measurements are determined separately for each feeder.

3.4.3 Sc. 3 - X Additional Measurements: all possible combinations of measurements located at *X* nodes are used as additional input data. The number of combinations is given by equation (8), where *N* is the total number of possible nodes to choose from. In this case *N* = 14, because there are 14 nodes with a measurement device, in addition to the low-voltage busbar of the transformer at node 48, see Fig. 2.

$$combinations = \binom{N}{X} = \frac{N!}{(N-X)!\,X!} \tag{8}$$

If any real PV measurements are included in a combination, these are used as replacement for the weather data, in order to improve the generation of the pseudo measurements according to Fig. 3.

3.4.4 Sc. 4 - All Node Measurements: in this scenario the measurements at all nodes are used as input data. This excludes the power flow measurements of each feeder. The generation of pseudo measurements is based on the PV measurements instead of weather data, as in 3.4.1.

4 Results

The DSSE is only performed for every quarter hour of each day within the studied week, in order to speed up the computation. However, the input data are still one-minute average values. It was found that this reduction in the sample size has only negligible influence on the results of this study, as shown in appendix A1.

4.1 Base Scenario - Sc. 1

The DSSE evaluation results of the base scenario, Sc.1, are shown in Fig. 4. The share of values inside the deviation ranges, marked by the grey background, are included in the legends. It can be observed that the deviations in voltage magnitudes are already very low, with this minimal measurement setup. However, the current magnitudes show much larger deviations between the recorded measurements and the DSSE results than the voltage magnitudes. Similar results were found for a medium-voltage system in [2]. When adding more real measurements to the input data of the DSSE, the goal should therefore be an improvement in the estimation of the current magnitudes.

4.2 Feeder Measurements Scenario – Sc. 4

One possible solution for improving the evaluation of current magnitudes is adding the power flow measurements for each feeder to the input data of the DSSE. However, this scenario has the disadvantage of using all the available current magnitude measurements as input data and as the evaluation basis. Therefore, a very low deviation of the current magnitudes is to be expected. The results shown in Fig. 5 meet this expectation. Furthermore, an improvement in the voltage magnitude deviations can be observed. The deviations are small enough to ensure a safe operation of the system, within its operational thresholds. The results of this scenario, coupled with the results of a scenario, which utilises all real measurements as input data for the DSSE, confirm the correct operation of the implemented DSSE algorithm, as described in appendix B.

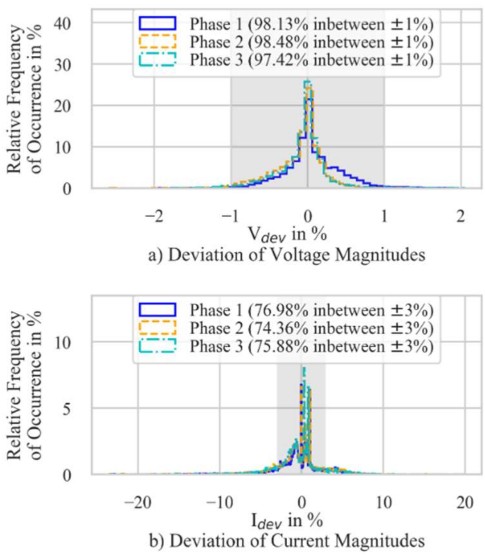

Fig. 4: DSSE evaluation results for the base scenario (Sc. 1) according to 3.4.1.

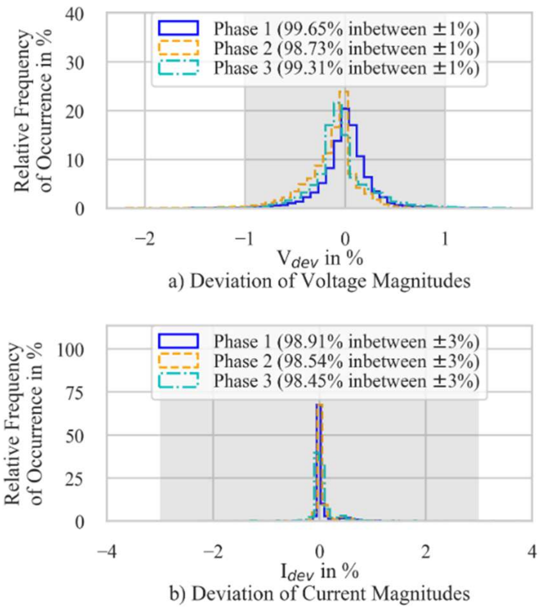

Fig. 5: DSSE evaluation results for the feeder measurements scenario (Sc. 2) according to 3.4.2.

4.3 X Additional Measurements – Sc. 3

In order to investigate the influence of different measurement locations on the current magnitude deviations, the feeder measurements are not included in the following scenario. The evaluation results for using one additional measurement device are condensed into Table 1. The table is sorted by the best evaluation results for the current magnitudes.

Table 1: DSSE evaluation results using one measurement device in addition to the measurements collected at the low-voltage busbar of the transformer (node 48).

Additional Measurement Location	Share of I_{dev} within ±3%	Share of V_{dev} within ±1%	Share of measured PV power
18	90.66 %	98.39 %	4.73 %
23	83.23 %	97.64 %	4.15 %
17	82.79 %	98.86 %	4.85 %
1	82.18 %	98.94 %	6.01 %
52	81.50 %	98.93 %	5.82 %
15	80.98 %	98.01 %	0.91 %
27	79,65 %	98.41 %	2.57 %
19	79.00 %	98.65 %	0 %
2	78.95 %	98.81 %	0 %
41	76.35 %	98.21 %	0 %
3	76.30 %	98.97 %	0 %
46	75.95 %	98.02 %	0 %
40	75.94 %	97.96 %	0 %
11	75.85 %	97.96 %	0 %

It can be seen that measurement locations at nodes without a PV measurement perform worse, compared to the other nodes. This was to be expected, because in this study the generation of pseudo measurements relies on a good estimation of the PV power output.

It is surprising that the measurement location at node 18 is far better than all the other possible locations, when it comes to the evaluation of the current magnitudes. This is due to a very high power consumption at node 18. During the night hours of the studied period (from 7:00 PM to 8:00 AM), the consumed energy at node 18 corresponds to 39.44 % of the whole low-voltage systems consumption. For comparison, at node 23 and 17 the share of consumed energy is only 0.80 % and 1.64 %. This unusually high demand in power is the reason for the big influence of measurement data from node 18 on the DSSE results. However, this kind of detailed information is usually not available, when deciding at which nodes to invest into measurement devices, in order to perform DSSE. The first measurement device installed in a new system should therefore be placed at a node with a PV system as a reference. Nodes with a high yearly energy demand should be preferred, if this information is available.
Table 2 summarises the results for the usage of two additional measurements. The table is also sorted by the best evaluation results for the current magnitudes and only the first ten entries are listed. All combinations of two measurement locations, excluding node 18, show worse results for the current magnitude deviations than using only the measurements from node 18. Overall, there is only a small benefit from using a second measurement. However, it can be observed that the accuracy of the voltage estimations benefits the most from measurements located in different feeders.

Table 2: DSSE evaluation results using two measurement devices in addition to the measurements collected at the low-voltage busbar of the transformer (node 48).

Additional Measurement Locations	Share of Idev within ±3%	Share of Vdev within ±1%	Share of measured PV power
18 & 1	92.31 %	99.62 %	10.74 %
18 & 17	92.09 %	99.48 %	9.58 %
18 & 23	91.75 %	97.82 %	8.87 %
18 & 41	91.40 %	98.60 %	4.73 %
18 & 52	91.30 %	99.71 %	10.54 %
18 & 15	91.29 %	98.23 %	5.64 %
18 & 3	91.13 %	99.76 %	4.73 %
18 & 27	90.85 %	98.61 %	7.30 %
18 & 2	90.85 %	98.62 %	4.73 %

4.4 All Node Measurements – Sc. 4

This scenario is considered as a comparison to the feeder measurements scenario. It has practical significance, because there are often no feeder measurements available for low-voltage systems. In the near future many distributed measurements from the grid could become accessible, e.g. through smart meters, to form a similar measurement setup. The DSSE evaluation results are shown in Fig. 6. It can be seen that using 14 instead of two additional measurement devices results only in a small increase of DSSE accuracy. However, the current magnitude deviations are deemed accurate enough to ensure a safe operation of the system, if a small additional error margin is considered for the operational thresholds.

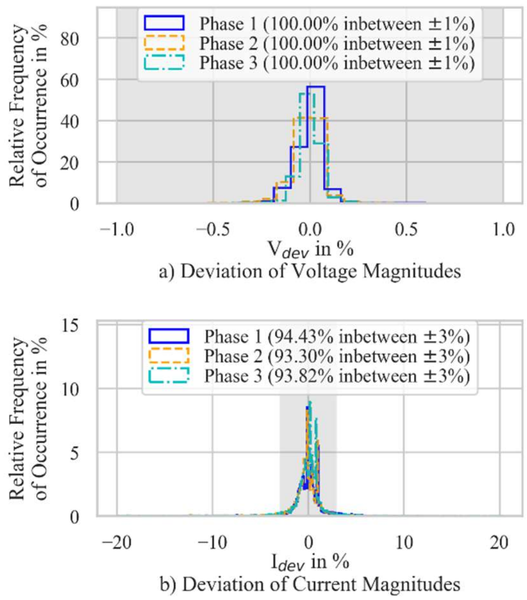

Fig. 6: DSSE evaluation results for the all node measurements scenario (Sc. 4), according to 3.4.4.

5 Conclusions

The evaluation of the performed DSSE shows that it is possible to estimate the system states of a real, radial low-voltage system with a reasonable amount of real measurement data. However, this requires a good mathematical model of the system and a correctly tuned weighting matrix R of the DSSE algorithm. The weight tuning process may require temporary calibration measurements and needs to be studied further.
The results show that it is possible to judge whether the operation of an unmeshed low-voltage system is within its thresholds or not, based on a minimal measurement setup, which uses only measurements from the low-voltage busbar of the transformer and the power flows of the connected feeders. The feeder measurements can be substituted with many distributed measurements from the grid, e.g. through smart meters. In this case a small additional error margin should be considered, in order to ensure the systems safe operation.
It becomes apparent that the estimations of the voltage magnitudes are more accurate than the estimations of the current magnitudes and therefore the resulting power flows.
Furthermore, it is shown that measuring the injected power of a reference PV system benefits the DSSE accuracy. It is also found that customers with high energy demands should be prioritised, when deciding at which locations of the system to invest into measurement equipment.
It is the authors assessment that the DSSE performed in this paper is accurate enough to use the results as a basis for higher-level control strategies of smart grid applications, such as determining the best ratio for a transformer with an on line tap changer or the curtailment of RES. A further increase in accuracy can be achieved through the usage of smart meter measurements, which need to be collected in near real time. Therefore, the upcoming challenges in the implementation of DSSE are heavily related to the connection and management of millions of data endpoints in the distribution systems, as well as the realistic modelling of these systems.

6 Appendices

A) Influence of sample size reduction on the DSSE evaluation

In order to reduce the computation times, the influence of reducing the sample size was investigated. The evaluation results shown in Fig. A1 are from a minutely performed DSSE over the studied time period of one week. The differences to the evaluation results of a DSSE performed for every quarter hour, as shown in Fig. 4, are negligible.

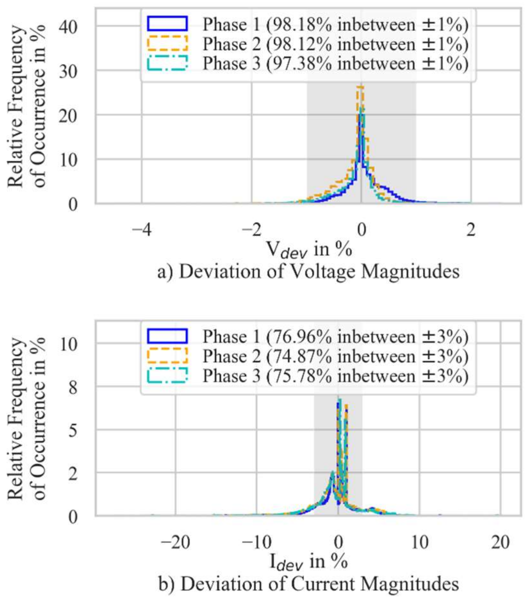

Fig. A1: DSSE evaluation results for the base scenario according to 3.4.1 with a higher sample size.

B) Correct operation of the DSSE algorithm

The evaluation results of a DSSE using all available measurements as input data are displayed in Fig. B1. These results show the correct operation of the DSSE algorithm, because the real measurements are estimated very accurately. This is due to the higher importance of real measurements in the weighting matrix *R*, compared to the pseudo measurements.

The deviations in the current magnitudes outside the ±3% range show that the measurements do not form a valid power flow with the used grid model, for approximately 1.5% of all timepoints. This is due to inaccuracies in the grid model, as well as errors in the measurement data. The errors in the measurement data are the most likely reason, because of the usage of minutely averaged values, instead of momentary measurements.

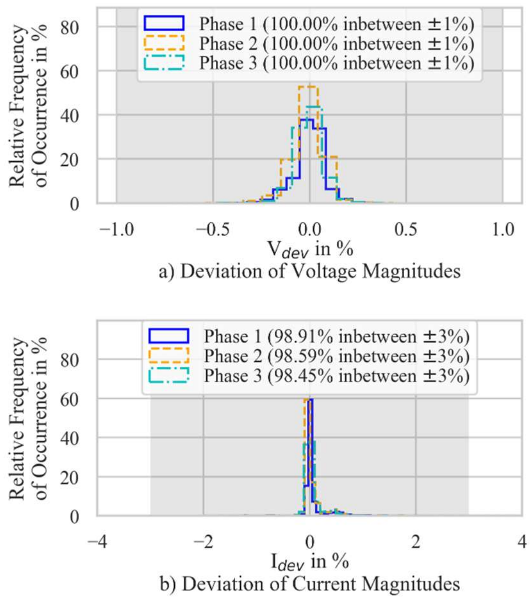

Fig. B1: Evaluation results for a DSSE using all available measurements as input data and as the evaluation basis.

7 References

[1] F.C. Schweppe, J. Wildes, "Power System Static-State Estimation, Part1 Exact Model", IEEE Transactions on Power Apparatus and Systems, Vol. PAS-89, No. 1, pp. 120-125, 1970.

[2] D. Groß et al., "Evaluation of a Three-Phase Distribution System State Estimation for Operational Use in a Real Medium Voltage Grid," 2019 IEEE PES Innovative Smart Grid Technologies Europe (ISGT-Europe), Bucharest, Romania, 2019, pp. 1-5.

[3] A. Primadianto, C. Lu, "A Review on Distribution System State Estimation," in IEEE Transactions on Power Systems, vol. 32, no. 5, pp. 3875-3883, Sept. 2017.

[4] R. Singh, B. C. Pal and R. A. Jabr, "Choice of estimator for distribution system state estimation," in IET Generation, Transmission & Distribution, vol. 3, no. 7, pp. 666-678, July 2009.

[5] Z. Jia, J. Chen and Y. Liao, "State estimation in distribution system considering effects of AMI data," 2013 Proceedings of IEEE Southeastcon, Jacksonville, FL, 2013, pp. 1-6.

[6] A. Alimardani, F. Therrien, D. Atanackovic, J. Jatskevich and E. Vaahedi, "Distribution System State Estimation Based on Nonsynchronized Smart Meters," in IEEE Transactions on Smart Grid, vol. 6, no. 6, pp. 2919-2928, Nov. 2015.

[7] T. Mota Soares, U. Bezerra, M. Tostes, "Full-Observable Three-Phase State Estimation Algorithm Applied to Electric Distribution Grids," in Energies. 12. 1327. 10.3390/en12071327, 2019.

[8] A. Abur, A. G. Exposito, "Power System State Estimation - Theory and Implementation," Marcel Dekker, 2004.

[9] M. L. Crow, "Computational Methods for Electric Power Systems," CRC Press, 2009.